EIC Detector R&D Progress Report

December 30, 2015

Project ID: eRD12

Project Name: Electron polarimetry, low Q^2-tagger, luminosity monitor

Period Reported: from July 2015 to December 2015

Project Leader: Elke Aschenauer

Contact Person: Elke Aschenauer, Richard Petti

Project members: BNL physics: Elke-Caroline Aschenauer, Alexander Kiselev, Richard Petti, William Schmidke; BNL-CAD: Vladimir Litvinenko, Vadim Ptitsyn, Dejan Trbojevic; BNL-Magnet Division: Brett Parker

Abstract

This document describes the progress made since the last July 2015 report [1] on the eRD12 research project on the development of an electron beam polarimeter, luminosity monitor and low Q^2-tagger projects and the general integration within the interaction region (IR). More information can be found in the eRHIC design study report [2]. The main focus of the recent work was on the study and integration of the electron polarimeter system.

1 Past

The goal for this period of review has been to develop a plan related to the electron polarimeter system at an EIC. A large portion of the work has been completed. This includes a literature search of existing and planned facilities making use of electron polarimetry, the writing of a Monte Carlo Compton event generator and writing code to assist in the analysis of the Compton events to extract an asymmetry. We have also performed studies to determine the statistics needed to achieve a 1% level of precision to the polarization measurement, which has a major impact on the choice of a laser system, which is also part of the ongoing study. Details will be discussed below.

1.1 Electron polarimeter overview

An electron polarimeter is essential to the physics goals of an EIC. Due to the expected high precision of the high luminosity collider, the required precision of the polarization measurements are of utmost importance. The polarization needs to be determined to better than 1% in order to make groundbreaking measurements. Physics measurements require longitudinal polarization of the electron beam (the spin of the electrons parallel to the electron momentum). At eRHIC, this will be achieved by spin rotator magnets installed before the interaction point (IP). Thus, there is a need for detectors to measure the longitudinal polarization fraction of the electron beam. Additionally, it is essential to measure the transverse component of the beam polarization to ensure that the spin of the electrons is fully rotated. This is not only necessary to quantify for any physics measurement, but can also assist in the tuning of the magnets to optimize the spin rotation during running.

The primary technology used by other experiments to determine electron beam polarization at the planned energy of operation of eRHIC is the measurement of asymmetries in Compton backscattering. In these measurements a laser impinges upon the electron beam, giving rise the the Comtpon scattering events. The laser is circularly polarized and the helicity state is flipped. The resulting asymmetry measured in the scattered electrons or photons from the event is related to the polarization of the electron beam (as well as the polarization of the laser beam). The asymmetry is defined as the difference in cross-section of the process between the two helicity states normalized by the total cross-section $\left(\frac{\sigma_{3/2}-\sigma_{1/2}}{\sigma_{3/2}+\sigma_{1/2}}\right)$. The longitudinal polarization gives rise to an energy asymmetry of the scattered particles A transverse polarization component gives rise to an energy dependent position asymmetry, due to the transverse component of the spin breaking the azimuthal symmetry. This can be seen from QED calculations, which have been put into a Monte Carlo generator to produce events for further study.

1.2 Requirements for the electron polarimeter

The following requirements guide the design and planning for the electron polarimetry system:

- Placement before the interaction point
- Placement after the spin rotators
- Measure polarization during normal operation (not destructive to the beam)
- Excellent precision to at least the 1% level
- Collect sufficient statistics on the order of a few minutes to measure the polarization of each cathode (linac-ring option) or bunch (ring-ring option)
- Measure both the longitudinal and transverse spin components

It is important to note that there are two design options being developed by CAD at BNL. One is the linac-ring design detailed in the eRHIC Design Study [2]. The second option is a ring-ring design. The requirements are similar to the polarimeter system for both options. Both options require spin rotator magnets to rotate the transversely polarized beam to longitudinal for physics as discussed in the document in the following sections.

1.3 Integration of the polarimeter system into the eRHIC machine lattice

Finding a suitable location for the polarimeter system is one of the major goals of the current study. This location has been identified, although the details of the machine lattice at this point have not been fully worked out. The polarimeter system needs to be placed after the spin rotators and preferably before the IP. The β function of the beam must also be small at the Compton interaction point. A natural location for the system is near the orbit shift that is planned which brings the electron beam into the IP. While the details are not worked out, the basic layout is shown in figure 1. The location of the orbit shift is a desirable location because the magnets present to achieve the shift will allow both the separation of the photons from the electron beam, as well as to act as a spectrometer for the scattered electrons. We are investigating installing detectors to register both the scattered electron and the photon to make the polarization measurement.

1.4 The physics of Compton scattering and the Monte Carlo generator

The scattering of polarized electrons from circularly polarized photons has been calculated in QED, resulting in analytic solutions. The analytic equations for the differential cross-section are summarized in equations 1-4 (assuming no crossing angle). These equations

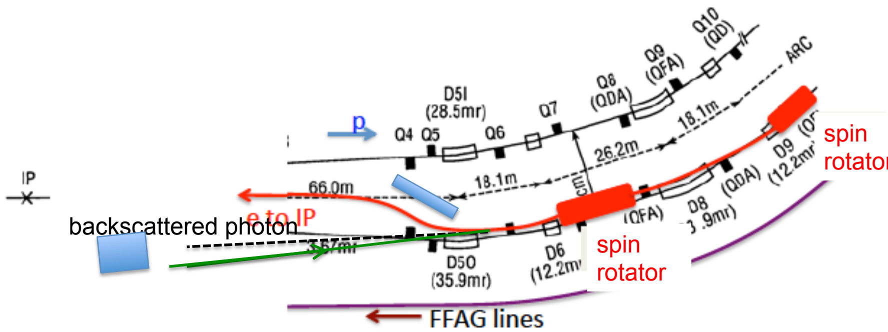

Figure 1: A schematic of the existing RHIC tunnel illustrating the approximate placement of the electron beam line (red line), its orbit shift to the IP, and the placement of spin rotator magnets (red boxes). Also illustrated is an approximate location for the polarimeter system, including the laser IP and electron and photon detectors (blue boxes).

form the basis for the Monte Carlo generator that is now being used to generate Compton events for detector simulations studies (some results shown below). The simulation incorporates both transverse and longitudinal polarization. The user can input the angle of the spin vector (Ψ), as well as the overall fraction of polarization. Other user inputs include the electron beam energy and the laser beam energy.

$$\frac{d^2\sigma}{d\rho d\phi} = \frac{d^2\sigma_0}{d\rho d\phi} \mp \mathrm{P_e P_\gamma} \left(cos\Psi \frac{d^2\sigma_1}{d\rho d\phi} + sin\Psi cos\phi \frac{d^2\sigma_2}{d\rho d\phi} \right) \tag{1}$$

$$\frac{d^2\sigma_0}{d\rho d\phi} = \mathrm{r}_0^2 a \left[\frac{(\rho(1-a))^2}{1-\rho(1-a)} + 1 + \left(\frac{1-\rho(1+a)}{1-\rho(1-a)} \right)^2 \right] \tag{2}$$

$$\frac{d^2\sigma_1}{d\rho d\phi} = \mathrm{r}_0^2 a \left[(1-\rho(1+a)) \left(1 - \frac{1}{(1-\rho(1-a))^2} \right) \right] \tag{3}$$

$$\frac{d^2\sigma_2}{d\rho d\phi} = \mathrm{r}_0^2 a \left[\rho(1-a) \frac{\sqrt{4a\rho(1-\rho)}}{1-\rho(1-a)} \right] \tag{4}$$

The cross-sections described by the equations are visually shown by the distributions in figures 2 and 3. From these plots, the energy asymmetry from longitudinally polarized beams (figure 2) and the position asymmetry in ϕ from transversely polarized beam (figure 3) becomes apparent.

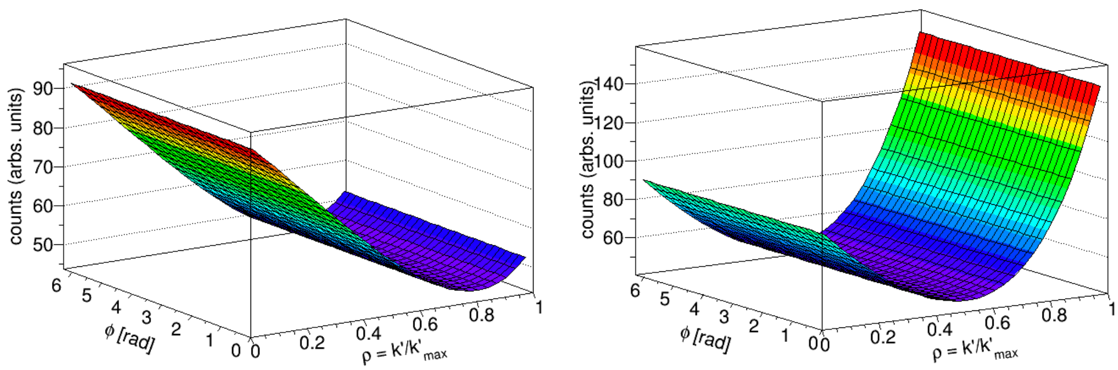

Figure 2: The differential cross-section distribution in photon energy, ρ, and azimuthal angle, ϕ, for a fully longitudinally polarized electron beam. The collision is for 20GeV electrons on 2.33eV photons. The two plots shows the polarized cross-section for each helicity state.

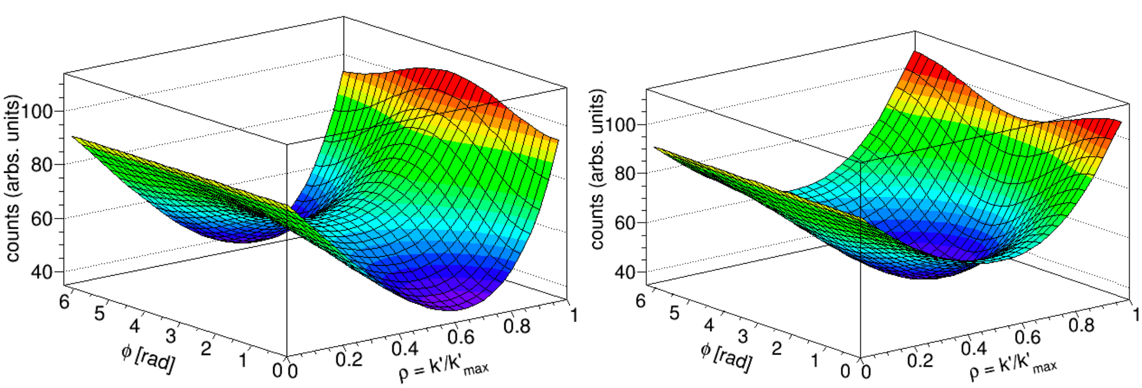

Figure 3: The differential cross-section distribution in photon energy, ρ, and azimuthal angle, ϕ, for a fully transversely polarized electron beam. The collision is for 20GeV electrons on 2.33eV photons. The two plots shows the polarized cross-section for each helicity state.

1.5 Polarimeter simulations

As stated, we desire to have devices to measure both the scattered electron and the scattered photon, and to measure both the longitudinal as well as the transverse polarization fraction of the electron beam. Since we do not have a detailed layout of the machine lattice at this point, we make some reasonable assumptions to be able to start the work and even investigate some requirements to the lattice configuration based on the needs of the polarimeter. For the electron measurement, we consider the measurement after the electron passes through a 2m long dipole magnet with a field of 0.2T. At this stage we are not considering synchrotron radiation background and so this consideration currently has no consequence on the photon measurement and efforts are mainly concerned with developing the software tools to carry out a more sophisticated analysis.

First we will discuss the simulations performed measuring the longitudinal polarization fraction. Let us also begin by considering the measurement of the scattered photon from the Compton process. At the moment we consider making the measurement in "single photon mode", meaning that we measure the energy of each individual photon that hits the calorimeter. This is the simplest configuration. The calorimeter in the simulation set up consists of square towers of 25mm face size and 200mm long. The material in the simulation is $PbWO_4$.

We measure the experimental asymmetry, A_{exp}, in this case by taking the number of photons as a proxy for the cross-section. Thus the asymmetry can be measured by calculating the quantity of equation 5 as a function of the photon energy, E_γ.

$$A_{exp} = \frac{N_{3/2} - N_{1/2}}{N_{3/2} + N_{1/2}} \tag{5}$$

Compton events for each helicity state have been generated in equal amounts (10,000 events each) and the results of the asymmetry is shown on the left side of figure 4. In this method, we fit the measured asymmetry distribution with the asymmetry calculated by QED (A_{theory}). The electron beam polarization fraction is then extracted using the relation $A_{exp} = P_e P_\gamma A_{theory}$, where we assume that the polarization of the laser (P_γ) is 100%. The right panel of the figure shows the ratio of the measured asymmetry, A_{exp}, to the calculated asymmetry, A_{theory}. The ratio is fit with a constant, representing the polarization of the electron beam. We extract one, which was the input to the simulation. This represents a proof of principle simulation and will form the basis for more detailed studies.

Next, we focus on simulation results using the measurement of the scattered electron to determine the longitudinal polarization. This method is a bit more involved than the previous consideration. In this measurement, we convert the energy asymmetry to a position asymmetry in the detected position of the electron via a dipole magnet as a spectrometer. The displacement of the electron hitting the detector after passing through the magnet is

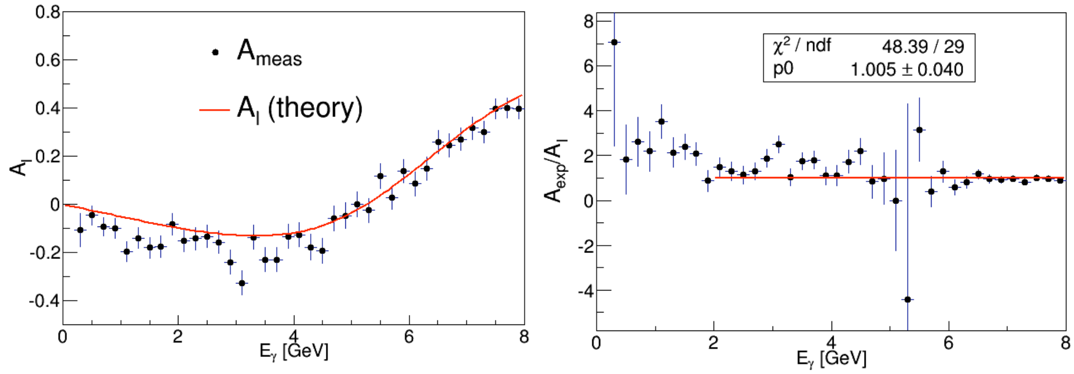

Figure 4: Left: The measured longitudinal asymmetry, A_{exp} from the simulation compared to the theoretical asymmetry, A_{theory}, shown by the red line. Right: The ratio of the measured to the theoretical asymmetry.

directly related to the energy of the scattered electron. A simple schematic of the simulation setup is shown in figure 5, where a strip detector is inserted in the simulation to register the electron hits.

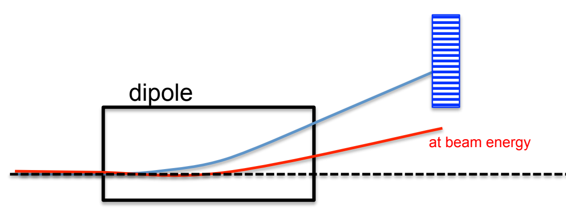

Figure 5: A simple schematic diagram of the simulation setup for the longitudinal asymmetry measurement from the scattered electron.

In this type of strip detector setup, the asymmetry can be measured in each strip separately. The asymmetry in each strip is calculated simply from the number of counts that strip registers in the two helicity states, see equation 6. In the equation, j represents the particular strip number.

$$A_{exp,j} = \frac{n_j^+ - n_j^-}{n_j^+ + n_j^-} \tag{6}$$

In order to connect the asymmetry as a function of strip position (or number) to QED calculations, one needs to convert the theoretical asymmetry originally calculated as a function of the photon energy to be as a function of strip position. This can be done, since we know the kinematics of the Compton process, as well as the strength of the magnetic field, the distance to the detector, and the width of the strips of the detector. The analytic expression relating the photon energy (expressed as ρ) and the displacement in x on the face of the detector has been derived and in this way we convert the original equation from QED to a form more useful for the experimental setup.

The main goal of the simulation currently is to determine the optimal distance to the detector, the strip pitch, and the desired laser power. All of these features combine to result in some statistics per strip, which propagates to the overall precision of the polarization measurement. As a concrete example, we look at a specific setup with a 0.5m drift distance between the end of the magnet and the detector and a 250μm strip pitch. Figure 6 shows the measured asymmetry as a function of strip number, along with the fit of the theoretical asymmetry. Note that in this simulation, the setup is superficial in that the detector sensor was placed directly in the line of the beam (which is why the numbering does not start at zero or one). This will be adjusted to be more realistic in the future, but for the present purposes leads to the necessity to limit the fit range as not all strips will be kinematically accessible. This is something that has been studied and will be discussed later. There is a single fit parameter in the theoretical asymmetry, which represents the polarization of the beam. A value of 0.8 is extracted, which is the input to this simulation.

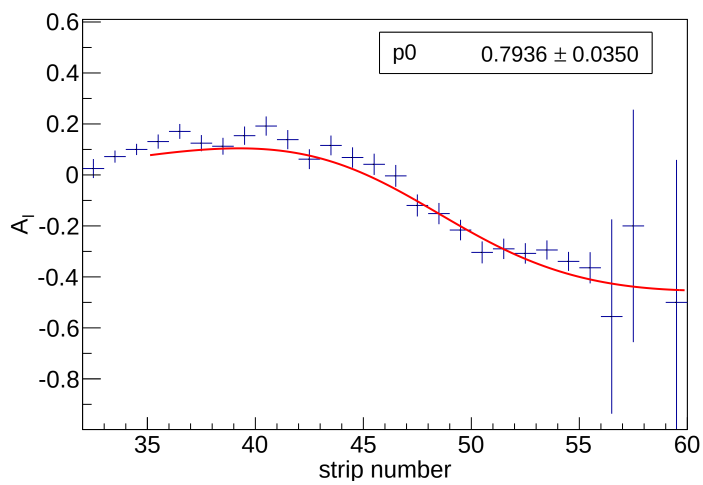

Figure 6: A simulation of the measured longitudinal asymmetry from measuring electrons from Compton scattering events. The red line is a fit to the theoretical asymmetry with a single fit parameter, the polarization fraction.

One of the goals of this study is to determine the statistics needed to get at least 1% precision on the polarization. The theoretical asymmetry distribution is used to generate fake data. We generate the asymmetry for each strip based on the theoretical asymmetry smeared by some statistical uncertainty. Here we focus on the 0.5m drift space setup,

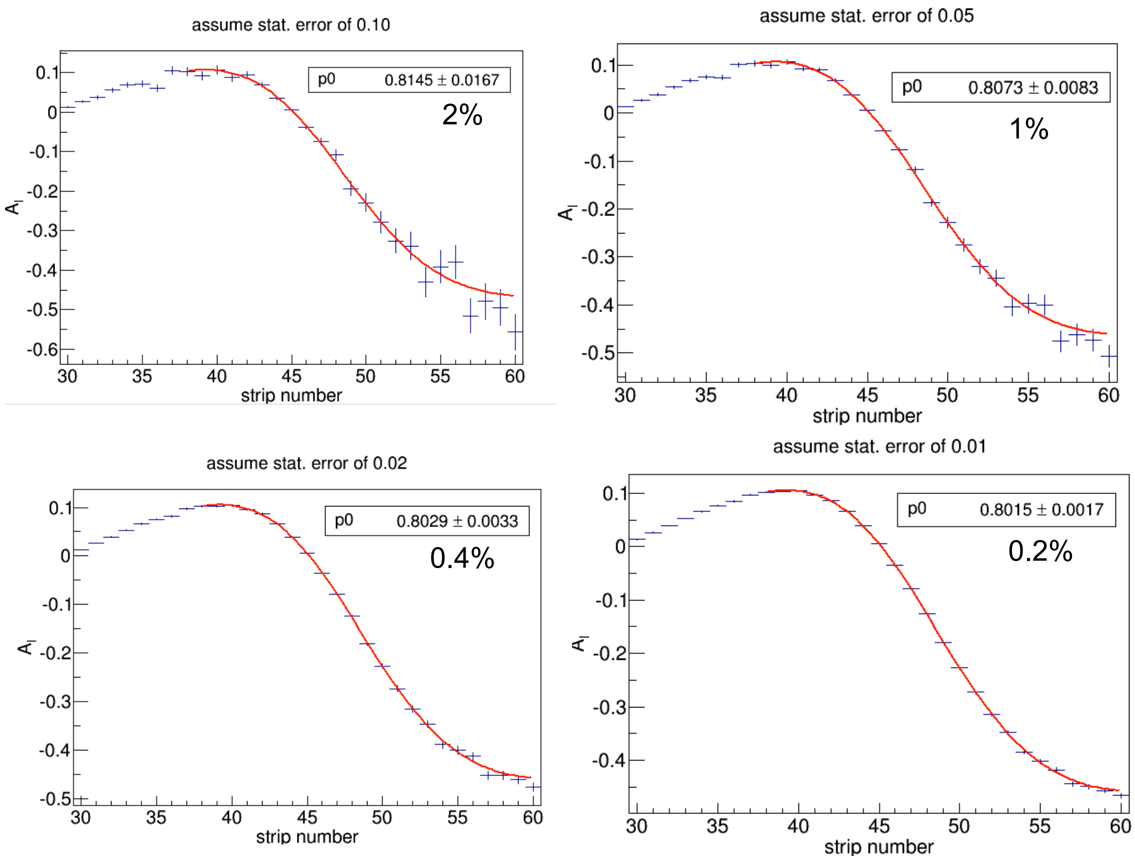

Figure 7: A study for the statistical uncertainty feeding into the uncertainty of the polarization measurement.

though this can be easily repeated for any drift distance. The difference will be in the number of points that enter the fit (assuming the strip pitch remains the same) since a larger drift leads to a larger spread in the hit distribution on the detector. To be a bit more realistic, the fits are truncated to simulate the fact that we cannot measure electrons all the way to the beam energy. Figure 7 shows some results from this study, with each panel representing the generated asymmetry with a different statistical precision. From the plots, it is observed that to have at least a 1% level of uncertainty on the polarization, we need roughly a 5% statistical uncertainty on the points of the experimental asymmetry. This translates to requiring roughly 1000 events per helicity state in each strip. For this particular setup, this means roughly 20,000 events total per helicity state. The details of how this information is translated to laser power requirements is still under investigation.

Now let us turn our attention to simulations regarding the measurement of the transverse polarization of the beam. These studies are still ongoing and are not ready for this report, but we expect to have some results to discuss in the presentation at the upcoming meeting at the end of January.

2 Future

The initial goals of the project are nearly complete. We now have a basic plan for the placement and detector geometry for the luminosity monitor, low Q^2-tagger, and electron polarimeter (as well as the forward proton tagger implemented as roman pots which was not part of this initial proposal). Apart from completing the polarimeter studies (transverse polarization measurement, laser requirements/considerations), the main focus in the remaining time is refining the simulation studies and more carefully consider backgrounds that the detectors may encounter. We will continue to move forward in conjunction with the machine development to come to a solution that will meet the physics goals and fully expect this study to be complete at the end of the proposed funding term (summer 2016).

3 Manpower

Manpower working on the project is summarized below, listed in alphabetical order, but separated by department.

- Elke Aschenauer - BNL physics. Provides project guidance and is the supervisor of the project.
- Alexander Kiselev - BNL physics. Provides software support.
- Richard Petti - post-doc at BNL working under the supervision of Elke Aschenauer. Performed the bulk of the work and works on the project full time.

- William Schmidke - BNL physics. Provides project guidance through expertise in polarimetry.
- Vladimir Litvinenko - BNL-CAD. Provides project guidance through expertise on the collider side. Facilitates machine related discussions.
- Brett Parker - BNL-CAD/Magnet division. Provides the magnet design of the interaction region.
- Vadim Ptitsyn - BNL-CAD. Provides project guidance and design of the spin rotator magnets.
- Dejan Trbojevic - BNL-CAD. Provides project guidance through expertise in the machine lattice design.

4 Publications

A conference proceedings from the POETIC 2015 conference summarizing this work will be published early 2016. The proceedings are being prepared and will be submitted in mid-January.

References

[1] https : //wiki.bnl.gov/conferences/images/4/4e/ERD12_report_2015 − 6.pdf

[2] http : //arxiv.org/ftp/arxiv/papers/1409/1409.1633.pdf